CHAPTER 50

Velocity Field under Plunging Waves

Akio Okayasu*, Tomoya Shibayama** and Nobuo Mimura***

ABSTRACT

    In order to clarify the characteristics of the velocity field in
the surf zone, three sets of detailed and precise two dimensional
laboratory experiments were performed. Spatial distributions and time
histories of velocity were measured by using a hot film velocimeter with
a split type probe or a two components laser doppler velocimeter for
regular wave conditions. Typical plunging breakers were formed during
the experiments. Based on the experimental results, a model was
investigated in order to estimate the two dimensional distribution of
the on-offshore steady current below the trough level.

1. INTRODUCTION

    The velocity field in the surf zone is much concerned with the
phenomena there. Therefore, it is a very important technical problem to
make it clear. The velocity field there is rather complicated because of
its non-uniformities in time and space. However, with the recent
development of the velocity measurement techniques, many researches have
been carried out to clarify the structure of the turbulent velocity
field in the surf zone by measuring the velocity itself [Sakai et
al.(1984), Aono and Hattori (1984), Nadaoka et al.(1986) and Mizuguchi
(1986)].

    Svendsen et al.(1978) separated the surf zone into three regions
which were an outer, inner and run-up region. In the outer region, rapid
transitions of wave shape occurs, particularly in case of plunging
breakers. Sawaragi and Iwata (1974) suggested the existence of a large
scale vortex formed just below the wave plunging and it is frequently
called "horizontal roller" or "plunging vortex". In the inner region,
the breaking wave propagates shoreward with deformation like a bore.
Both such bore-like waves and plunging vortexes seem to give strong
effect to the generation of turbulence in the surf zone. On the other
hand, the existence of "undertow" caused by the mass transport of
breaking waves has recognized for many years [see e.g. Hansen and
Svendsen (1984)].

  * Graduate Student, Dept. of Civil Eng., Univ. of Tokyo, Bunkyo-ku,
    Tokyo, 113 JAPAN
 ** Associate Professor, Dept. of Civil Eng., Univ. of Tokyo, Bunkyo-ku,
    Tokyo, 113 JAPAN
*** Associate Professor, Dept. of Civil Eng., Ibaraki Univ., Hitachi,
    Ibaraki, 316 JAPAN

    Thus we will consider the following factors: (1) plunging breakers,
(2) bore-like waves and (3) undertows, which characterize the velocity
field in the surf zone in comparison with that in the offshore region.
One of the objectives of the present study is to clarify these
characteristics of the velocity field through detailed and precise
laboratory experiments.

    Then, applying the results from these experiments, we will
formulate a model to estimate the two dimensional distribution of on-
offshore steady current below the trough level.

2. EXPERIMENTS

2.1 Experimental Arrangements and Procedures

    Three individual laboratory experiments were performed in a two
dimensional wave flume which was 23m long and 0.8m wide and two
different beach profiles were used, a step type and a constant slope of
1/20.

    For the case 1, the step type beach profile was used for the sake
of grasping the behavior of the plunging vortex. The profile consisted
of a 1/10 slope and a flat bed. The reasons why we chose this type of
beach topography were to fix the breaking point of each wave and to
reserve an enough region for the measurement. The beach topography is
shown in Fig.1. The measuring area was from 0.5cm to 14.5cm above the
bottom and 80cm long in an on-offshore directed vertical plane. The
measuring points were arranged to make 2cm grids.

    For the case 2 and 3, a constant slope of 1/20 was used to measure
the whole area of the surf zone. And it was expected that the effects of
the bore-like waves and the undertows would be revealed. The measuring
areas were about 250cm long in both cases, but the arrangements of
measuring points were different. The 2cm grids arrangement was taken for
the case 2. The lowest points were 7mm above the bottom and the detailed
arrangement is shown in Fig.2. On the other hand, for the case 3, an
arrangement which was rough in the horizontal direction and close in the
vertical direction was used for the purpose of detailed measurements of
the vertical profiles of the undertow. The measuring points were
arranged with 10cm distance in the on-offshore direction and 2.5-10mm
distance in the vertical direction. On every measuring line, at least
seven measuring points were set below the trough level. The lowest ones
were 2mm above the bottom. The arrangement is shown in Fig.3 which is
enhanced in the vertical direction.

    The x-axis and z-axis were set to be shoreward and vertically
upward, respectively. The origin of the coordinates in the case 1 was on
the bottom as shown in Fig.1 and in the case 2 and 3, the shorelines at
the still water levels were set to be the origins. In the case 3, the
breaking point was at x_b=-250cm (indicated by "A" in Fig.3), the
plunging point at x_p=-215cm ("B" in Fig.3) in the coordinates. After
breaking, the wave propagates shoreward forming successive vortexes on
the water surface. And the point where this vortex become a rather
stable "surface roller" was around x_1=-170cm ("C" in Fig.3). The point

where the surface roller began to attenuate was at $x_d = -80cm$ ("D"). The mean shoreline was at $x_s = 50cm$ in the case 3. In the case 1 and 2, the breaking points were at $x_b = 10cm$, $-225cm$ (indicated by "A" in Fig.1 and 2), and the plunging points at $x_p = 24cm$, $-162cm$ ("B"), respectively.
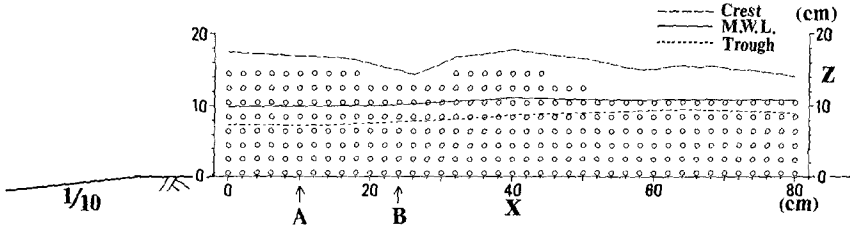
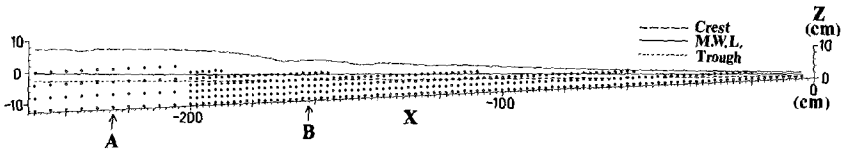Fig.1   Measuring points arrangement for case 1
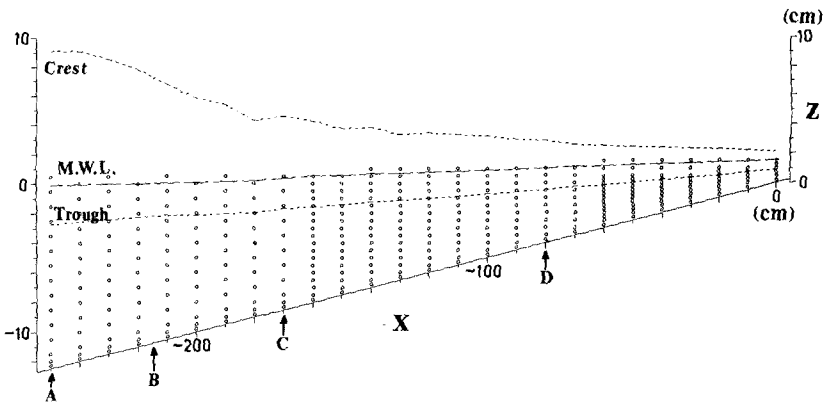
Fig.2   Measuring points arrangement for case 2

Fig.3   Measuring points arrangement for case 3

The experimental conditions are listed in Table I. In the table, T is the wave period, h_i the water depth in the offshore uniform depth region, H_i the wave height there, H_0/L_0 the deep-water wave steepness, H_b/h_b the depth wave height ratio at the breaking point.

Table I   Experimental Conditions

case	beach profile	T(s)	h_i(cm)	H_i(cm)	H_0/L_0	H_b/h_b
1	step	1.55	40.0	6.95	0.0201	1.02
2	const. slope	1.50	40.0	7.36	0.0226	0.901
3	const. slope	1.50	36.4	8.15	0.0249	0.954

2.2 Data Processing and Analysis

A hot film velocimeter with a split film probe (H.F.V.) was used to measure the histories of two dimensional velocity vectors for the case 1 and 2. And a two components laser doppler velocimeter (L.D.V.) was used for the case 3.

By using the H.F.V. we can obtain two components of velocity, which are one component of velocity histories with the plus or minus sign and an absolute value of the other component. Therefore, we cannot get full information about the signs of two components. In the case 1, the sign of the on-offshore component of the velocity was not determined. Therefore, we made an assumption that the surface profile and the on-offshore velocity are in phase. So the sign of the velocity was reversed once in every wave period according to the surface profile. In the case 2, we measured the velocity two times, once for the on-offshore and the other time for the vertical direction to avoid such an uncertainty. In case of using the L.D.V., we can get full information of velocity for two components and there is no problem like that.

The velocity data were sampled every 10ms (for the case 1 and 3) or 12ms (for the case 2) and were converted into digital data. The surface elevation data were also taken simultaneously. The equi-phase-mean values of the velocity over 30 (case 1 and 2) or 100 (case 3) periods were calculated. Each wave period was divided into 150 (or 125 for the case 2) intervals and the equi-phase-mean value was obtained as an average of the velocity values at the same phase of every wave. The turbulence component was determined as the deviation from the equi-phase-mean value.

2.3 Experimental Results

The steady currents, the spatial distributions and time histories of equi-phase-mean velocities, vorticities and turbulent intensities were obtained. Fig.4 gives an example of the results for the case 1. The equi-phase-mean velocity field, the vorticity field and the turbulent intensity field at the time immediately after the wave plunging are shown in the figures. A large scale vortex can be observed obviously by the velocity vectors in the figure. And the high vorticity and turbulent intensity regions are in good agreement with the velocity vectors which suggest the existence of the plunging vortex.

Fig.5 is the successive figures of the equi-phase-mean velocities after plunging. The process that the first plunging pushes up the neighboring water body and the second plunging occurs in a smaller scale is shown. The plunging vortex formed by the first plunging does not move according with the crest and goes downward. The contour maps of the turbulent intensity at the same phases are shown in Fig.6. The high turbulent region goes ahead slowly behind the wave crest and spreads, then dissipates.

Based on these facts, it can be concluded that the generation of the plunging vortex has much influences on the characteristics of the velocity field and is much concerned with the energy dissipation process under plunging waves. Up to now, the velocity field in the surf zone were often described as a form in [steady current] + [wave component (periodic component)] + [turbulence]. This time, however, the measured results point out that the periodic component consists of the irrotational wave component and the organized rotational motion due to
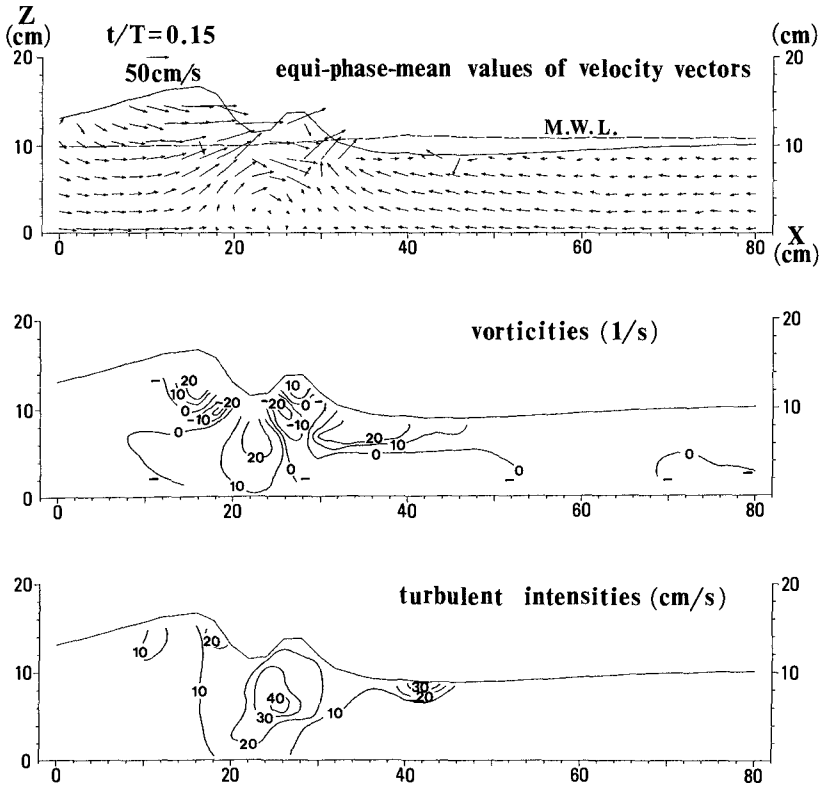

Fig.4   Velocities, vorticities and turbulent intensities
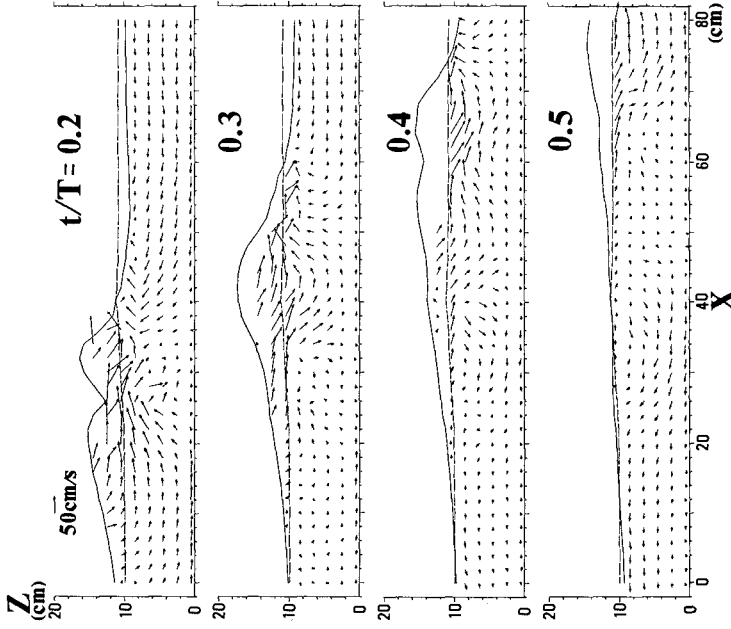   immediately after wave plunging

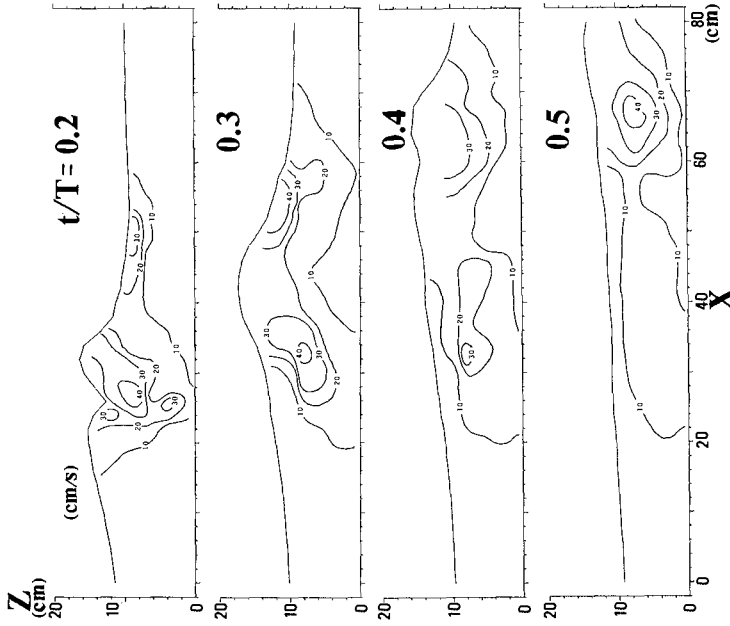Fig.5 Equi-phase-values of velocity
vectors for case 1

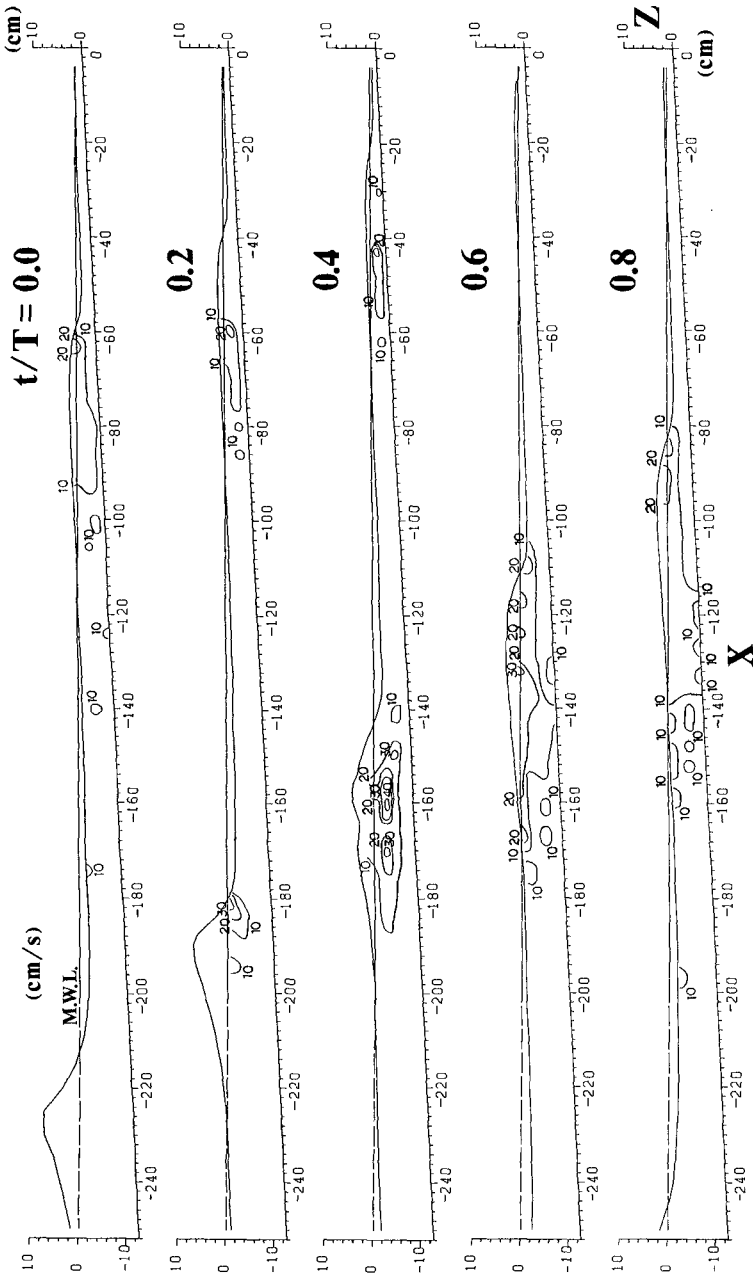Fig.6 Distributions of turbulent
intensities for case 1

Fig.7 Distributions of turbulent intensities for case 2

the wave plunging. And it can be said that the plunging vortex is an important fluid motion existing between the wave motion and the turbulence or the steady current. Therefore, we propose that the velocity field in the surf zone should be divided into four components as [steady current] + [non-rotating wave motion] + [organized vortex motion] + [turbulence].

Fig.7 gives the successive contour maps of the turbulent intensity for the case 2. The figure shows a high turbulent region in front of the wave crest. It should be noticed that this turbulence is caused by the vortex motion as described by Nadaoka et al.(1986) which is formed there. And in the figure the turbulence spreads downward, so it should influence the turbulent flow field there and the bottom boundary layer. The figure indicates another turbulent region from $x=-40$cm to $x=-80$cm at the phases 0.0-0.6. As this high turbulent region stays there after the wave crest passes, it can be said that this turbulence is due to the interaction between the bore-like wave and the return flow from the swash zone. The high turbulent region caused by the wave plunging is also ascertained in this figure.

Fig.8 shows the steady current distribution for the case 3. Observing this figure, we found that the bottom boundary layer develops at the breaking point, but in the region where the bore well develops the bottom boundary layer does not develop any more. And we considered that it is due to the turbulence created by the bore-like waves. The large gradient of the profiles of the undertow shows that large shear stress works at the mean water level.
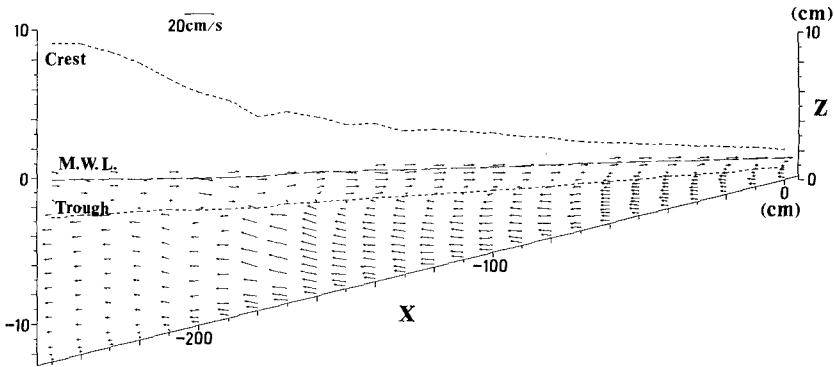

Fig.8   Steady current distribution for case 3

3. MODELING OF UNDERTOW

3.1 On-offshore Variation of Vertically Averaged Undertow

The estimation of the steady current distribution is very important for evaluating such as the convective diffusion of materials or the

sediment transport in the surf zone. However, the steady current
distribution in the surf zone is much different from that of any wave
theory solved in the invisid condition. The surface roller which is
formed just in front of the crest of the bore-like wave propagating in
the surf zone affects the mass flux balance and the turbulence
generation as shown in the section 2. Now in this section, taking the
case 3 as an example, we will try to formulate a model to calculate the
profile of the undertow that is the steady current distribution below
the trough level.

For the reasons mentioned above, when we consider the mass flux
above the trough level which is transported by the bore-like wave, we
should take into account both the contribution from the wave component
and the contribution from the surface roller. For the wave component,
Isobe et al.(1979) reported that the wave component of the velocity in
the surf zone fits well to the velocity calculated by the stream
function method which is presented by Dean (1965). Accordingly, the
stream function method was used for estimating the wave component. We
divided the bore-like wave into two parts, the surface roller and the
wave component which can be explained by the stream function method.
Then as shown in Fig.9, we supposed that the velocity inside the surface
roller equals to the wave celerity c in the same manner as Svendsen
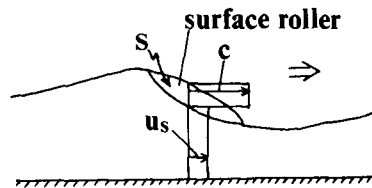(1984) did.

Fig.9 Assumption of velocity distribution of bore-like wave

As the sum of the mass fluxes by the surface roller and the wave
component balances to the offshore steady current below the trough, the
vertically averaged undertow U_c is calculated by using the projected
area S of the surface roller to the xz-plane, the height of the trough
d_t and wave length L as

$$U_c = U_s + U_r = U_s + \frac{S}{d_t L} c \, , \qquad (1)$$

where U_s and U_r are the contribution to U_c from the surface roller and
the wave component, respectively.

Then we nondimensionalized the projected area S of surface roller
by the wave height H and the wave length L. Further more introducing the
parameter k,

$$
k = \begin{cases}
0 & (x \leqq x_p) , \\
\dfrac{x_p - x}{x_p - x_i} & (x_p < x \leqq x_i) , \\
1 & (x_i < x \leqq x_d) , \\
\dfrac{x - x_s}{x_d - x_s} & (x_d < x \leqq x_s) ,
\end{cases} \tag{2}
$$

for convenience, as a degree of the development of the surface roller, we presented S as

$$
S = kAHL . \tag{3}
$$

Thus Eq.(1) becomes

$$
U_c = U_s + \frac{kAH}{d_t} c , \tag{4}
$$

where A is a constant and was taken to be 0.06 for the case 3 in order to fit the measured value U_m. And we chose the wave celerity c as

$$
c = \sqrt{g (h + H)} , \tag{5}
$$

based on the solitary wave theory, where g is the gravity acceleration and h the mean water depth.

The comparison between the calculated velocity U_c by Eq.(4) and the measured velocity U_m is shown in Fig.10. As they are in good agreement in the whole area of the surf zone, it can be said that our treatment in which the size of the surface roller is expressed by the parameter k, is adequate.
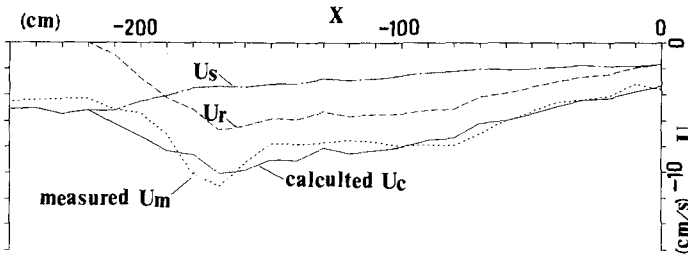

Fig.10 Calculated value of vertically averaged steady current U_c and measured value U_m

3.2 Vertical Variation of Undertow

Svendsen (1984) calculated the vertical variation of the on-offshore steady current by using the eddy viscosity model. But the magnitude of the eddy viscosity was left unknown and the agreement with the measured data near the bottom was not good enough. In the present

study, we will try to estimate the vertical profiles of the undertow with the eddy viscosity ν_t, which is directly calculated from the measured data, the Reynolds stress and the on-offshore velocity.

By using the eddy viscosity model, the relation between the mean shear stress $\bar{\tau}$ acting on the horizontal plane and the steady current U is

$$\bar{\tau} = \rho\nu_t \frac{\partial U}{\partial z} \; . \tag{6}$$

If the $\partial\bar{\tau}/\partial z$ takes a constant value, Eq.(6) can be written as

$$\frac{\partial\bar{\tau}}{\partial z} = \frac{\partial}{\partial z}\left(\rho\nu_t \frac{\partial U}{\partial z} \right) = \alpha_1(x) = \text{const.} \tag{7}$$

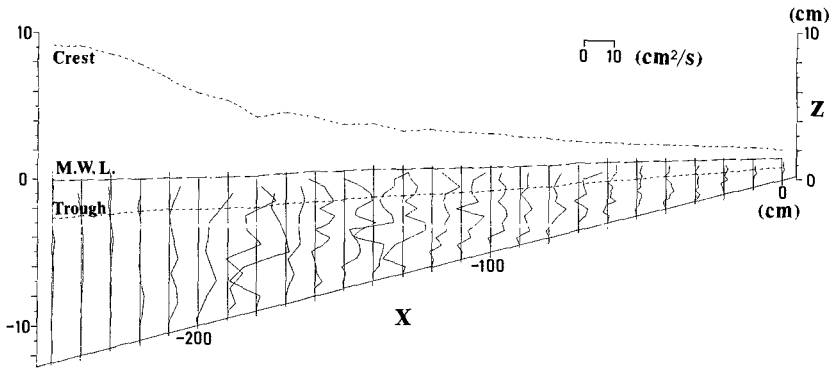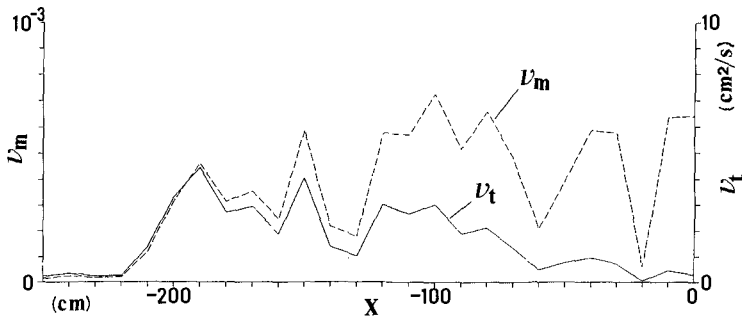Fig.11   Distribution of mean eddy viscosity
averaged over one wave period

Fig.12   On-offshore distribution of vertically averaged eddy
viscosity ν_t and nondimensional value ν_m

Fig.11 shows a distribution of the mean eddy viscosity by averaging the eddy viscosity of each phase over one wave period. In the figure it is possible to take it being constant along a vertical line except close to the bottom. From this reason we made a rather bold assumption that the mean eddy viscosity is constant over the depth. Eq.(7) can be reformed as

$$\frac{\partial \overline{\tau}}{\partial z} = \rho \nu_t \frac{\partial^2 U}{\partial z^2} \ . \tag{8}$$

Furthermore, we obtain

$$\frac{\partial^2 U}{\partial z^2} = \frac{1}{\rho} \frac{\partial \overline{\tau}}{\partial z} \ / \ \nu_t \ = \ \alpha(x) \ . \tag{9}$$

The on-offshore variation of the nondimensional value ν_m which is calculated from the vertical average of ν_t below the trough level divided by c and d_t, is shown in Fig.12. It is seen that ν_m progressively increases after the plunging point and then becomes rather stable around 0.005-0.006 in $x>x_i$ (~170cm) except some fluctuations. Therefore, we supposed that

$$\nu_t \ = \ 0.005{\sim}0.006 \ cd_t \ . \tag{10}$$

On the other hand, the nondimensional value obtained from α_l divided by $\rho c^2/d_t$ can be supposed to be a constant value in $x>x_i$. The value α_l in Eq.(7) can be expressed as

$$\alpha_l \ = \ 0.0012 \ c^2/d_t \ . \tag{11}$$

Consequently, we denote α in Eq.(9) as

$$\alpha \ = \frac{1}{\rho} \ \alpha_l / \nu_t \ \approx \ 0.2 \ c/d_t^2 \qquad (\ x \ > \ x_i \ ) \ . \tag{12}$$

As α is very small in offshore side of the plunging point, it was taken to be 0 in that region. And we linearly interpolated it between the plunging point and the point where a stable surface roller is formed $(x=x_i)$. As a result we obtain

$$\alpha \ = \ 0.2 \ k'c/d_t^2 \ , \tag{13}$$

where the parameter k' is

$$k' \ = \ \begin{cases} 0 & (\ x \leqq x_p \ ) \ , \\ \dfrac{x_p \ - \ x}{x_p \ - \ x_i} & (\ x_p \ < \ x \ \leqq \ x_i \ ) \ , \\ 1 & (\ x_i \ < \ x \ \leqq \ x_s \ ) \ . \end{cases} \tag{14}$$

For the bottom boundary condition, we thought it is appropriate to give it by the slip, i.e., no shear stress condition inside the high turbulent region, because the bottom boundary layer does not develop

there as we mentioned in the section 2. However, the velocity field near
the breaking point is not so turbulent that it is better to give 0 to
the eulerian steady current on the bottom U_b, as suggested by Isobe
(1982). Accordingly, using the bottom steady current U_{b0} which is solved
with the slip condition and k in Eq.(2), we calculated U_b as

$$U_b = k U_{b0} . \qquad\qquad (15)$$

Using these three conditions which are, (1) the mean value U_c of
the steady current below the trough level, (2) the ratio α of the eddy
viscosity ν_t to $\partial \bar{\tau}/\partial z$ and (3) the steady current U_b at the bottom, we
can solve Eq.(9). And putting $z'=z+h_0$ where h_0 is the still water level
measured from the bottom, we obtain

$$U = \frac{1}{2}\alpha z'^2 + 2(1-k)\ U_{b0}\ \frac{z'}{d_t} + k U_{b0} , \qquad\qquad (16)$$

where

$$U_{b0} = U_c - \frac{1}{6}\alpha d_t^2 .$$

The comparison between the steady current distribution calculated
by Eq.(16) and the measured value of it is shown in Fig.13. The
calculated and the measured value fit well except in the region between
the breaking point and the plunging point. One of the reasons of the
discrepancy is that the linear interpolation for α and U_b is not
adequate, and another reason is that we neglected the influence of the
plunging vortex formed near the plunging point. Anyway we can say that
it is difficult to describe the flow field in the outer breaking region
where such a violent transition as plunging takes place. And the
disagreement near the bottom is due to the assumption of the constant
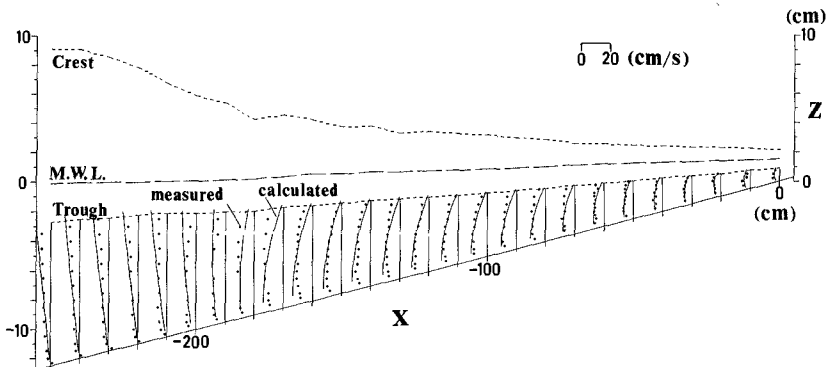eddy viscosity near the bottom.

Fig.13 Distribution of calculated steady current
        and measured value

4. CONCLUDING REMARKS

    Through detailed and precise laboratory experiments, we clarified
the characteristics of the velocity field in the surf zone with plunging
breakers. Then we proposed that the velocity field can be divided into
four components, the steady current, wave component, organized vortex
motion and turbulence. And this organized vortex motion is an important
fluid motion existing between the wave motion and the turbulence.

    Based on the laboratory results, we investigated a model for the
estimation of the vertical profile of the undertow available in whole
the surf zone. We found that the mean steady current over the depth can
be divided into the contribution from the wave component and that from
the surface roller. The onshore mass flux by the surface roller can be
expressed quantitatively by an empirical constant multiplied by the wave
length and the wave height and a simple linear interpolation of the
constant value. In the region where the surface roller well develops,
the vertical variation of the undertow can be estimated by supposing a
constant eddy viscosity over the depth and a no shear stress condition
on the bottom. On the other hand, the bottom steady current near the
breaking point can be taken to be 0. The calculated steady current
distribution fits well to that from measured data all over the surf
zone, however the agreement is not so good near the bottom and in the
outer breaking region.

5. ACKNOWLEDGMENT

    The authors thank to Mr. Y. Higuchi who assisted the experiment of
the case 2.

6. REFERENCES

Aono, T. and M. Hattori (1984) : Experiments on coherent structures of
large scale turbulence under breaking waves, Proc. 31st Japanese Conf.
Coastal Eng., pp.6-10. (in Japanese)

Dean, R.G. (1965) : Stream function representation of nonlinear ocean
wave, J. Geophysical Res., Vol.70, No.18, pp.4561-4572.

Hansen, J.Buhr and I.A. Svendsen (1984) : A theoretical and experimental
study of undertow, Proc. 19th ICCE., pp.2246-2262.

Isobe, M., N. Fukuda and K. Horikawa (1979) : Two dimensional experiment
on velocity field in the surf zone, Proc. 26th Japanese Conf. Coastal
Eng., pp.41-45. (in Japanese)

Isobe, M. (1982) : Study on drift velocity at the bottom in and near the
surf zone, Proc. 29th Japanese Conf. Coastal Eng., pp.140-144. (in
Japanese)

Mizuguchi, M. (1986) : Experimental study on kinematics and dynamics of
wave breaking, Abstracts 20th ICCE., pp.75-76.

Nadaoka, K., M. Hino and Y. Koyano (1986) : Turbulent flow field structure of breaking waves in the surf zone, Abstracts 20th ICCE., pp.71-72.

Sakai, T., I. Sandanbata and M. Uchida (1984) : Reynolds stress in surf zone, Proc. 19th ICCE., pp.42-53.

Sawaragi, T. and K. Iwata (1974) : Turbulent effect on wave deformation after breaking, Costal Eng. Japan, Vol.17, pp.39-49.

Svendsen, I.A., P.A. Madsen and J.Buhr Hansen (1978) : Wave characteristics in the surf zone, Proc. 16th ICCE., pp.520-539.

Svendsen, I.A. (1984) : Mass flux and undertow in a surf zone, Coastal Eng., Vol.8, pp.347-365